A novel approach to the estimation and application of the wear coefficient of metal-on-metal hip implants

Francesca Di Puccio[1*] and Lorenza Mattei[2]
[1-2] Department of Civil and Industrial Engineering, University of Pisa, Largo Lucio Lazzarino 2, 56122 Pisa, Italy
[1] dipuccio@ing.unipi.it
[2] l.mattei@ing.unipi.it

[*]Corresponding author: email: dipuccio@ing.unipi.it, +39 050 2218076

Abstract
A novel approach is proposed to estimate and model the wear of metal-on-metal hip implants. The approach is based on two distinct wear coefficients for the head and cup, derived from separate measurements on the two components. This is in contrast to the usual assumption that a single wear coefficient (k) is valid for both bodies. Actually, the head and cup do not wear equally; thus, assuming equal wear leads to predictive errors. Additionally, in most papers, k is chosen considering only implant materials while neglecting geometry and testing conditions. It is suggested that experimental procedures designed for hip implants should measure the head and cup volume losses separately and that wear maps should be provided to validate numerical models.

Keywords: wear coefficient; Archard wear law; wear predictive model; hip replacement

1. Introduction

Currently, wear is considered one of the main concerns in hip replacements (HRs), not only for the most widespread metal-on-plastic (MoP) implants but also for the new generation of metal-on-metal (MoM) couplings [1,2]. In fact, in MoM devices, typically made of CoCrMo alloy, wear is associated with the release of toxic metallic ions, which have been shown to promote inflammation, reduce cell activity and cause pseudo-tumors [3].

Numerical HR wear prediction is an attractive tool for investigating long-term wear at low cost and has been pursued by many researchers in the last decade, e.g., [4-7]. However, the reliability of these predictions primarily depends on a dimensional wear coefficient k, the evaluation of which is a critical issue, being based itself on experimental tests and numerical simulations. In fact, the wear coefficient k for a hip implant is generally estimated by matching numerical and experimental wear volumes, with the former being calculated by means of a suitable numerical model, while the latter is obtained by joint simulator tests [5,6], typically reproducing simplified gait cycles. Usually only the total or cup volume loss is measured. Hence, a single wear coefficient is estimated for the implant, whose use in a predictive model implies that the two components are affected by the same wear amount (i.e. same volume loss) or that only one of them becomes worn, as in MoP implants. However, this is not true in general. Moreover, an average estimate of k over a high number (hundreds of thousands) of cycles is obtained. Indeed, k can vary during a wear test, as well as during a single gait cycle, because it depends on the lubrication regime, which, in turn, is affected by the implant geometry, bearing materials and loading conditions [2,8]. Therefore, k is notably not constant for a given material coupling or for a specific implant; rather, it depends on the test conditions. Thus, the reliability of a wear prediction starts with the reliability of the experimental and numerical simulations of the implant real-like working conditions. On the other side, it is worth noting that the validation of a predictive wear model cannot be based on the wear volumes used to estimate k, but should be obtained by the wear maps. To the authors best knowledge none of the studies in the literature provides such a validation; only in [6] Liu et al. comment this point and report a qualitative comparison of the numerical wear maps and implant pictures.

Although many experimental data on total wear volumes of hip implants are available in the literature, only in a small number of cases the values of k are provided, perhaps because their calculation requires a numerical model. However, such values are typically scattered, spanning from 10^{-9} to 10^{-7} mm^3/(N m), which can be partly attributed to the different loading conditions.

In this study, a set of wear volume data for metal-on-metal hip implants was collected from the literature and the respective wear coefficients were calculated by means of a model developed by the authors and presented in [7,9]. A novel approach is proposed for HR wear assessment that is based on two distinct measurements/wear coefficients for the head and cup. Because the formulation is rather general, the approach can be applied to other tribological systems as well. On the basis of the numerical simulations, the following issues have been addressed: (i) comparison between a single k value for the entire implant vs. double cup/head coefficients, and an analysis of the corresponding wear predictions; (ii) analysis of the experimental wear data obtained from different hip simulators, using one single numerical model (i.e., eliminating the variability on the k estimations due to the model itself); (iii) evaluation of the effects of the implant characteristics and the test conditions on k.

However, besides the numerical application, the aim of the present study is mainly focused on the theoretical aspects of the estimation and application of the wear coefficient for metal-on-metal hip implants, i.e.:

- to propose an approach based on the double measurements of volume losses of the two components, both in

experimental and numerical simulations;
- to underline the specificity of the wear coefficients with respect to the simulated coupling and working conditions;
- to stress limitations and validation steps of predictive wear models.

The paper is organized as follows. Background on the basic relationships for k evaluation is presented followed by a description of the hip simulators to summarize loading and kinematic conditions of the wear tests. Next, the novel approach is proposed, and several fundamental equations are derived for the estimate of the separate wear coefficients for the head and cup. Such simulations reveal the effects of the novel approach in wear predictions as consequences of the use of the two values of k and underline the influence of geometrical and testing conditions on the wear coefficients estimations.

2. Background on the Wear Coefficient Evaluation in Hip Replacements

The estimation of the wear coefficient is usually based on the Archard wear law, which is valid when abrasion and adhesion are the main wear mechanisms. The law states that the volume loss V is proportional, via k, to the product of the normal contact force L_N and the sliding distance s:

$$V = k\, L_N\, s\,. \tag{1}$$

Thus, the wear coefficient can be estimated by inverting Eq. (1) and experimentally measuring the wear volume ($V = V^{exp}$), i.e.,

$$k = V^{exp} \Big/ \left(L_N\, s\right). \tag{2}$$

Equations (1-2) represent simple expressions suitable for pin-on-plate wear tests, where the contact force is constant, the relative motion is translational (although sometimes it is also used in pin-on-disk tests) and the contact pressure can be assumed to be uniformly distributed over the contact area.

To take into account a cyclic variation of the loading and kinematic conditions, for a translational motion, an improved version of Eq. (2) can be adopted

$$k = V^{exp} \Big/ \int_{\gamma} L_N(s)\, ds \tag{3}$$

where L_N is integrated over the force track γ, i.e., the track drawn on the counter face over a motion cycle by the force application point and s is the arc length along γ. The integral in Eq. (3), as well as the product $L_N\, s$ in Eq. (2), are found to represent the work performed by frictional forces, scaled by the coefficient of friction.

2.1. Wear coefficient evaluation from hip simulators

Unfortunately, for hip wear tests, such equations become more complex because the load is not constant, the contact pressure not uniform and the kinematics three-dimensional. In fact, each contact point P of the cup/head describes its own relative trajectory γ_P with respect to the other element (head/cup) and is subjected to a time-varying pressure during a test cycle. Denoting by s the arc length along γ_P, the contact pressure can be written as $p(P,s)$ and the following expression of k can be obtained

$$k = V^{exp} \Big/ \int_{A} \int_{\gamma_P} p(P,s)\, ds\, dA \tag{4}$$

where A is the area of the head or cup. In fact, the integral in the denominator, again the work performed by frictional forces divided by the coefficient of friction, can be evaluated considering P belonging to the head or cup, indifferently. However, such a calculation can be difficult to perform because it requires the knowledge of the function $p(P,s)$. For example, in [10], this equation was applied to MoP implants, assuming that the contact area was equal to the cup area and adopting a simplified expression of the local instantaneous contact pressure. Unfortunately, such simplifications cannot be applied to MoM implants, where the contact area is usually much smaller than the cup surface and moves over it. A more accurate assessment of k can be obtained if a finite element (FE) model is available; in this case, the integral in Eq. (4) is obtained numerically and k is estimated using a trial-and-error procedure by matching the predicted numerical total wear volume with the experimental one. Note that a reliable evaluation of k requires the FE model to simulate correctly the testing conditions, which can differ from simulator to simulator, as described in the following section.

Being a general definition, Eq. (4) can be applied to all implant typologies, both MoM and MoP, improving the traditional definition of Eq. (2) and the Saikko's method [10]. Note that the experimental wear volume V^{exp} in Eqs. (2-4) is the total volume loss of the coupling.

Another type of useful information of the wear process is the local wear depth at each point of the mating surfaces, which can be obtained by a numerical model and is also measured by surface profilometers. When only one element of the contact couple undergoes wear, as in MoP implants, the linear wear depth $h(P)$ at each point P of the worn surface is given by

$$h(P) = k \int_{\gamma_P} p(P,s)\, ds \tag{5}$$

In addition,

$$k \int_A \int_{\gamma_P} p(P,s)\, ds\, dA = \int_A h(P)\, dA \qquad (6)$$

Finally, note that, according to experimental observations, MoM implants typically show wear trends such as the one reported in Fig. 1; thus the wear process is usually described by two values of the wear coefficient: one higher for the initial running-in (RI) phase and the other lower for the steady state phase, denoted as k_{ri} and k_{ss} respectively.

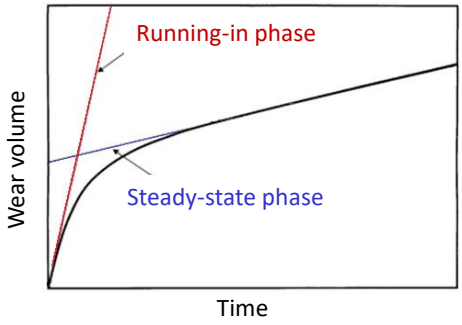

Fig. 1 Qualitative trend of the volumetric wear vs. time for MoM hip implants.

2.2. Hip simulators

Experimental wear tests on hip implants are typically performed using hip wear simulators, i.e., devices able to generate loading and kinematic conditions similar to those experienced *in vivo* by the hip joint. In most cases, hip simulators reproduce simplified gait cycles, as walking is considered the most common daily activity and thus the reference working condition. Wear tests can last several months, corresponding to 10-20 Mc (1 Mc= 10^6 cycles) performed at 1 Hz frequency.

The state of the art of the hip simulators includes many types of test rigs [11], both academic and commercial, which can differ in load type, kinematics, cup position (i.e., anatomical A or inverted NA) and orientation (i.e., inclination and anteversion), lubricant type (i.e., bovine serum, or synthetic ones). Specifically, the load can be applied to the head or the cup, and its line of action can be fixed or mobile. The load history/waveform, according to *in vivo* measurements [12], is generally characterized by a double peak during the stance phase, followed by a constant value during the swing phase (Fig. 2-a, b). The minimum (L_{min}) and the maximum (L_{max}) load values typically limit the working cycle within the range 0.1-3 kN. In contrast, the gait kinematics involves the hip spherical motion characterized by the sequence of flexion-extension (FE), abduction-adduction (AA) and internal-external (IER) rotations. Hip simulators can include all or only some of the motion components. In both cases, the angles and the rotations sequence must be specified. The motion can be assigned to a single component (cup/head) or separately to both (e.g., FE(h) + IER(c)) (Fig. 2-a, c). As an example, Fig. 2 describes the loading and kinematic conditions applied in the Prosim simulator [6]. The variability of the test conditions can be regarded as one of the causes of the high dispersion of the wear volumes found in the literature [7,9]. This high dispersion is even more evident for MoP implants, due to the cross-shear effect [9,13,14].

Wear tests in hip simulators can provide many useful pieces of information on the wear process, such as wear volumes (e.g., by means of gravimetric measurements of the implant or head/cup mass loss using accurate analytical balances) and linear wear maps of the head and cup surfaces (e.g., using co-ordinate measuring machines). The latter are very meaningful because they can provide information on the component and regions more prone to wear. Unfortunately, in most studies, only the total volumetric wear is reported, and, to the best of our knowledge, no quantitative wear maps can be found in the literature.

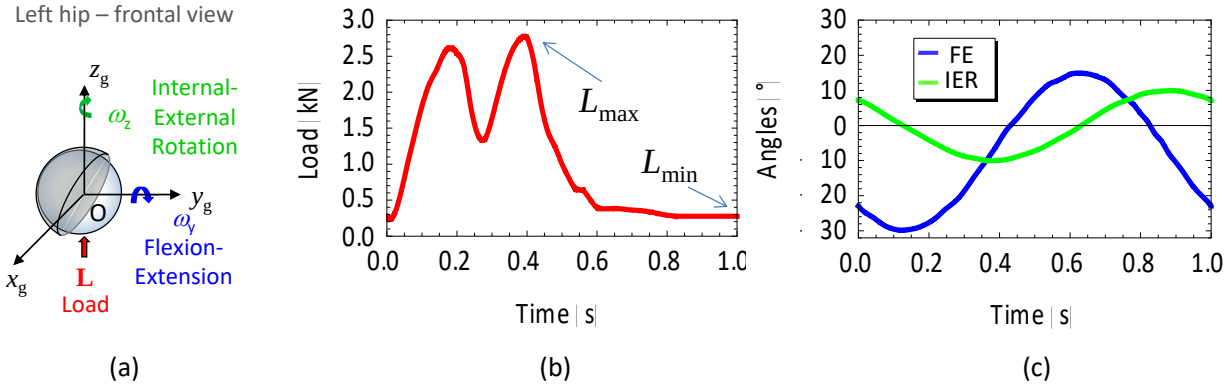

Fig. 2 a) Scheme of the implant in a fixed frame with the representation of thel load **L**, *and the angular velocities of the head (*$\boldsymbol{\omega}_y$*) and of the cup (*$\boldsymbol{\omega}_z$*). (b) Load profile and (c) FE and IER angles values, in a simplified gait cycle.*

(b) and (c) are typical trends of the Prosim simulator, with FE applied to the head and IER to the cup [6].

3. Novel Approach to Wear Coefficient Evaluation and Application

As highlighted above, the experimental wear volume V^{exp} in Eqs. (2-4) is the total volume loss of the coupling from which a unique k value can be obtained. As far as hip implants are concerned, such value can be used to compare the wear generated by different joint simulators and to correlate the *in vivo* and the *in vitro* wear rates. However, by the application of a single k value, it is not possible to determine how the total volume is distributed between the two mating elements. Usually, in these cases, it is assumed that V^{exp} is attributed to a single body or divided equally between the two bodies, that is, they are supposed to have the same wear loss. However, we highlight that, in the latter case, the wear distribution over the mating surfaces can be different in the two bodies [7,9]. In fact, the linear wear depth in the head and cup can be calculated according to the revision of Eq.(5)

$$\begin{aligned} h(P_c) &= \frac{k}{2}\int_{\gamma_c} p(P_c,s)ds \\ h(P_h) &= \frac{k}{2}\int_{\gamma_h} p(P_h,s)ds \end{aligned}, \tag{7}$$

where quantities referring to cup and head are denoted with the subscripts '*c*' and '*h*'; note that a halved wear coefficient is used with respect to Eq. (5). This point is important, as frequently the total wear coefficient is used both for one and two worn bodies.

When the experimental volumetric wear of both cup and head are available, two values of the wear coefficient can be calculated, that is

$$\begin{aligned} k_c &= V_c^{exp} \Big/ \int_{A_c}\int_{\gamma_c} p(P_c,s)\, ds\, dA \\ k_h &= V_h^{exp} \Big/ \int_{A_h}\int_{\gamma_h} p(P_h,s)\, ds\, dA \end{aligned} \tag{8}$$

and Eqs. (7) are replaced by the following ones

$$\begin{aligned} h(P_c) &= k_c\int_{\gamma_c} p(P_c,s)ds \\ h(P_h) &= k_h\int_{\gamma_h} p(P_h,s)ds \end{aligned} \tag{9}$$

Again the integrals in Eq. (8) can be evaluated considering P belonging to the head or to the cup indifferently, i.e.,

$$\int_{A_h}\int_{\gamma_h} p(P_h,s)\, ds\, dA = \int_{A_c}\int_{\gamma_c} p(P_c,s)\, ds\, dA \tag{10}$$

By comparing Equations (4), (8) and (10), the following relationship can be obtained

$$V^{exp}/k = V_c^{exp}/k_c = V_h^{exp}/k_h = \int_{A}\int_{\gamma_P} p(P,s)\, ds\, dA = \tilde{V} \tag{11}$$

where a scaled wear volume $\tilde{V}$ is introduced.

By using the following

$$V^{exp} = V_h^{exp} + V_c^{exp} \tag{12}$$

it is straightforward to determine that the total wear coefficient is the sum of wear coefficients of the two bodies

$$k = k_h + k_c \tag{13}$$

Equation (13) can be considered as a general result, although it is rarely found explicitly in other research articles.

It can be worth observing that this approach assumes a uniform k over each one of the articulating surfaces, i.e. k does not vary from point to point. While this is generally accepted for MoM implants, it is not true MoP replacements, where the modification of the molecular orientations of Ultra High Molecular Weight Polyethylene under multi-axial sliding conditions causes an anisotropic wear behavior of the cup, known as cross-shear [14].

Additionally, as already mentioned, k is considered time independent or piecewise constant in time (k_{ri} and k_{ss}), with consequent piecewise linear volumetric wear, according to the qualitative trend in Fig.1.

4. Numerical Wear Model and Simulations Plan

4.1. Wear model

The wear model used in the present study for calculating the wear coefficients is derived from the one presented by the same authors in [7,9] for a single k value. The model exploits an analytical formulation based on a robotics approach and was implemented in Mathematica®. The following simplifying hypotheses were assumed:

- abrasion and adhesion are the main wear mechanisms, which enables the Archard wear law to be adopted;
- the geometrical variation does not affect the contact mechanics because only the initial running-in phase is

simulated, i.e., $k=k_{ri}$;

- the contact is frictionless, because the friction has been demonstrated not to modify significantly the contact pressure and the total wear volumes (less than 3%) [7]; however it is taken into account in k.

To briefly summarize the model, only the main steps are reported. Three coordinate reference frames are introduced to describe the two implant components: two mobile ones (on both cup and head) and one fixed, denoted by g (Fig. 3). The coordinates of a generic point P_c/P_h of the cup/head at a given instant are obtained through rotation matrices between the frames ($\mathbf{R}_{gc}$, $\mathbf{R}_{gh}$), i.e.,

$$\begin{aligned}[P_c(t)]_g &= \mathbf{R}_{gc}(t)[P_c]_c \\ [P_h(t)]_g &= [O_h(t)]_g + \mathbf{R}_{gh}(t)[P_h]_h\end{aligned} \tag{14}$$

where O_h is the head center, whose position depends on the load direction defined by the unit vector $\boldsymbol{\lambda}$

$$[O_h(t)]_g = \frac{cl}{2}[\boldsymbol{\lambda}(t)]_g \tag{15}$$

where cl is the diametrical clearance.

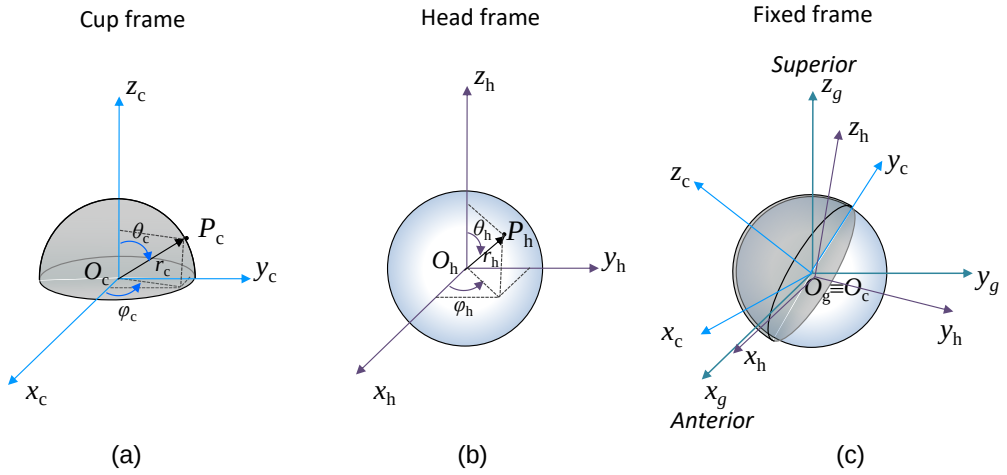

Fig. 3 Points of the cup (P_c) (a) and head (P_h) (b) in their local cartesian frames and indication of their spherical coordinates (r_c, θ_c, φ_c) and (r_h, θ_h, φ_h), respectively. Head and cup position in the fixed frame, in the reference configuration (null rotation angles) (c).

The kinematic conditions of the simulator can be introduced in the model through the rotation matrices and load vector, obtaining the relative trajectories γ_P of the each point, and the law of motion $s(t)$. In this way, the wear volume is conveniently calculated adopting the local instantaneous form, obtained by replacing the dependence on the arc length with that on time , that is

$$V = k \int_{A\gamma_P} \int p(P,s)\, ds\, dA = k \int_{A}^{T} \int_{0} p(P,s(t))\, |\mathbf{v}(P,t)|\, dt\, dA \tag{16}$$

where $\mathbf{v}(P,t)$ is the relative sliding velocity between the elements of the contact pair ($ds=|\mathbf{v}(P,t)|\, dt$), and T is the cycle period, typically assumed equal to 1 s. The Hertz formulas are used to calculate the contact pressure $p(P,s(t))$, adopting a suitable equivalent elastic modulus estimated by fitting analytical results on FE analyses of the implants.

Although limited to running-in phase simulations without a geometry update, the developed model allows rapid k evaluations (one analysis takes less than a few minutes) and hence avoids the high computational costs typical of FE wear models. In addition, the powerful symbolic calculus capability of Mathematica® can improve certain of the discretization limitations of the finite element method.

4.2. Simulated cases

In this study, the above mentioned model was used to estimate the wear coefficients of MoM implants from the wear volume data taken from the literature. For this purpose, a survey of the experimental wear studies was performed, and a wide dataset of hip simulator test conditions with the correspondent wear results were collected. Note that many of these studies do not provide all the data enabling their simulation (e.g., the load/angle curves, simulator characteristics, etc. are not specified); thus, in this paper, only a subset of ten cases was considered.

To investigate the role of implant geometry on wear, studies on both total hip replacements (THRs) [8,15] and hip resurfacing replacements (HRRs) [6,16,17] were chosen, characterized by different values of head diameter (d_h) and diametrical clearance (cl), as reported in Table 1. The tested implants were in CoCrMo alloy, generally with high carbon content (HC) (>0.2%) which guarantees a higher wear resistance. They were manufactured both as wrought (W) and cast (C), which however has been demonstrated to affect the running-in wear only slightly [18]. Moreover, all these selected cases were studied using the same hip simulator, the Prosim, which is clearly described in many studies, e.g., in [6]. In such apparatus, flexion-extension (FE) and internal-external rotation (IER) are assigned to the head and the cup,

respectively, whose angle curves are depicted in (Fig. 2-c). The load is applied to the head and thus continuously changes direction (load vertical for null FE angle). A Paul load type (Fig. 2-b) is simulated, with L_{min} and L_{max} being dependent on the test case and exhibiting values in the range of 0.1–3 kN. The lubricant used in these studies was diluted newborn bovine serum (NBS), in some cases supplemented with sodium azide (NaN_3), to retard bacterial growth, and ethylene diamine tetracetic acid (EDTA), to inhibit the deposit of proteins on the bearing surfaces (see Table 1). It is worth noting that the lubricant type and its protein content play a main role in the tribological behaviour of the coupling.

The wear data in Table 1 refer to the running-in phase because the numerical model, as already mentioned, does not take into account the geometry update. Note that the duration of the running-in phase is a critical issue because of the high dispersion of the experimental data. To obtain uniform wear data from different literature studies and perform a comparative analysis, a reference period of 1 Mc (10^6 cycles) was considered. Indeed this assumption is commonly accepted in the literature and is in agreement with half of the simulated studies (cases 5-9). For cases with an RI duration different from 1 Mc, the volume rates reported in Table 1 were calculated by properly scaling the given wear volume by the correspondent RI period, i.e., 2 Mc and 0.5 Mc for cases 2-4 and case 10, respectively. The only exception is case 1, for which a steady condition was not achieved even after 5 Mc of the wear test [8], for which a period of 2 Mc was assumed, as was assumed in [8] for other HRs without a RI phase. By analyzing Table 1, the total wear volume rates are found to be dispersed in the ranges of 0.13–2.25 and 1.13–2.58 mm^3/Mc for the THRs and HRRs, respectively. Note that only the three test cases 5, 6 and 10 reported distinct wear volumes for the head and cup, exhibiting higher values for the head, particularly in case 6.

The selected cases also facilitate the analysis of the sensitivity of k to the implant geometrical features and test conditions. For example, the effect of the head diameter can be evaluated by comparing case 1 vs. cases 2-4 for THRs [8] and case 7 vs. case 8 for HRRs [16]. However, the effect of the clearance can be analyzed by comparing cases 2-4, which tested implants with the same head size (d_h = 36 mm) but different cl (105 –143 μm), under the same working conditions. The effect of the load is highlighted in the study [15] (case 5 vs. case 6), where two identical implants were tested under two different load regimes/levels. In addition, the repeatability of the experimental wear data is verified by the comparison of test cases 8 and 9, which were tested under almost identical conditions.

Case	**THR/ HRR**	d_h	cl	***Materials & manufacturing***	***Lubricant***	$L_{min} - L_{max}$	V_h	V_c	V_{tot}	**Ref.**
		(mm)	(μm)			(kN)	(mm^3/Mc)			
1	THR	28	62.5	CoCrMo alloy, HC–W	25% NBS , 1.2g/l NaN_3, 0.325 g/l EDTA	0.3 – 3	-	-	2.25	[8]
2		36	143				-	-	1.76	
3		36	124				-	-	1.41	
4		36	105				-	-	1.16	
5		28	60	CoCrMo alloy, na – W	25% NBS, 0.1% (w/v) NaN_3	0.1– 2	0.08	0.05	0.13	[15]
6		28	60			0.28 – 2	1.57	0.46	2.03	
7	HRR	38.5	111	CoCrMo alloy, HC - C	25% NBS, 0.1% (w/v) NaN_3, 15.46 g/l proteins	0.28 – 3	-	-	2.58	[16]
8		54.5	126				-	-	1.15	
9		54.5	100	CoCrMo alloy, HC - na	25% NBS	0.28 – 2.8	-	-	1.2	[6]
10		49.8	236	CoCrMo alloy, HC – C	NBS, 2g/l NaN_3 20g/l proteins	0.3 – 3	0.78	0.34	1.13	[17]

Table 1 Simulated cases: geometrical properties (head diameter d_h, diametrical clearance cl); implant material of both head and cup: metal alloy, carbon content (high carbon content, HC) and manufacturing process (wrought, W, or cast , C); lubricant characteristics: serum type and concentration(v/v), eventual additives (e.g. NaN_3 and EDTA) and protein content; load range ($L_{min} – L_{max}$) and volumetric wear rates ($V_{h/c/tot}$ for the head, cup and whole

implant, respectively) for the running-in phase.

5. Results and Discussion

Numerical wear simulations of the ten cases listed in Table 1, provided the scaled volumes $\tilde{V}$ in Eq. (11) at 1 Mc. By comparing such values with the experimental ones, k estimations were obtained both for the head/cup and the entire implant according to Eqs. (4) and (8). Wear coefficients were estimated by this method and used to evaluate the correspondent numerical wear maps, according to Eqs. (7) or (9).

The main results are summarized in Table 2. Note that maximum wear depths (h_{max}) were calculated using k_h and k_c where available, whilst using k in all the other cases.

Case	THR/ HRR	k	k_h	k_c	h_{h_max}	h_{c_max}
		(10^{-8} mm^3/(N m))			(µm @ 1 Mc)	
1	THR	9.44	-	-	34.91	19.14
2		5.74	-	-	33.67	14.14
3		4.63	-	-	24.72	10.75
4		3.83	-	-	18.35	8.30
5		0.67	0.41	0.26	2.46	0.87
6		9.42	7.30	2.12	49.93	8.11
7	HRR	7.89	-	-	28.69	13.58
8		2.51	-	-	8.16	3.46
9		2.60	-	-	7.23	3.31
10		2.62	1.78	0.84	18.00	3.30

Table 2 Main results: estimations of the running-in phase wear coefficients of the entire implant (k) and the single head (k_h) and cup (k_c) components, and the maximum wear depths (h_{h/c_max}) at 1 Mc.

5.1. Estimation of the head and cup wear coefficients

The innovative aspects of this study consist of the estimation of the distinct wear coefficients for the head and cup, both affected by wear in MoM implants, and of the evaluation of how such an approach can affect numerical wear predictions. The values of k_h and k_c were estimated for the three available cases, i.e., cases 5, 6 and 10, and compared to the traditional $k/2$ obtained according to Eq. (13). To ease the comprehension of this point, the results are also plotted in Fig. 4. For all the simulated cases, the values of k_h were higher than those of k_c, up to even more than three-fold (see case 6), and hence were higher than $k/2$, that is, the average of the two. This is in agreement with experimental data ($V_h > V_c$) and could be explained by considering the simulated test conditions: the load being applied and fixed to the head causes it to wear more than the cup. Such an effect is evident in the cup/head wear maps predicted using the novel k_h and k_c and were plotted in Figs. 5-a and 5-b for the THR (case 6) and HRR (case 10), respectively: in both cases the head is characterized by linear wear values that are much higher compared to the cup ones. Moreover, the head exhibited a well-defined circular worn area, whilst the cup exhibited a stretched one, both consistent with the contact force trajectory on the bearing surfaces. To highlight the consequences of the novel approach on the wear predictions, the wear maps of cases 6 and 10 were computed assuming $k_c=k_h=k/2$ also, as shown in Figs. 5-c and 5-d, respectively. The comparison of the wear maps at the top and at the bottom of Fig. 5 (5a vs. 5c, 5b vs. 5d) confirmed that the adoption of a single wear coefficient for the two elements produced lower linear wear depths for the head and higher ones for the cup. The percentage errors in the prediction of the maximum values of the linear wear depth for the head and the cup were of approximately -36% and 122%, respectively, for case 6, and approximately -26% and 56% for the head and the cup, respectively, for case 10. Thus, the assumption of the implant wear volume being equally distributed between the head and cup, which is widely accepted in the literature, strongly affects the numerical wear predictions and introduces significant errors.

During the operation of a hip implant, an important wear redistribution mechanism among the head and cup occurs, which depends on the working conditions. To improve the numerical wear predictions, this relevant aspect should be considered both in the k estimation and in the wear modeling, which translates into evaluating and using different wear coefficients for the head and the cup.

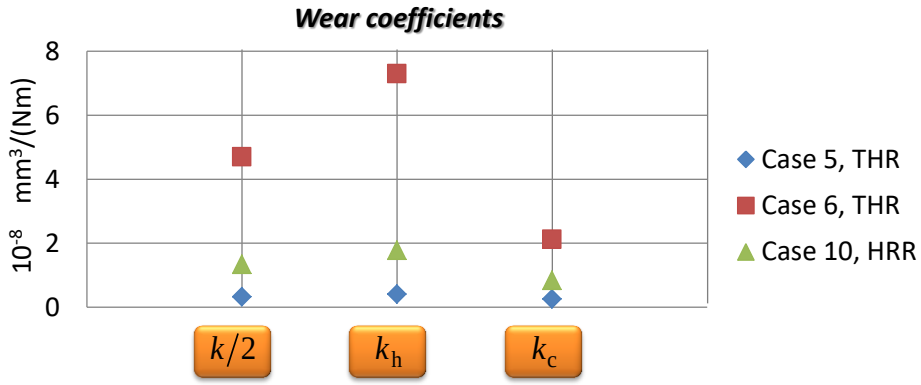

Fig. 4 *Comparison of the total/cup/head wear coefficients (k, k_c, k_h respectively). The simulated cases are defined in Table 1.*

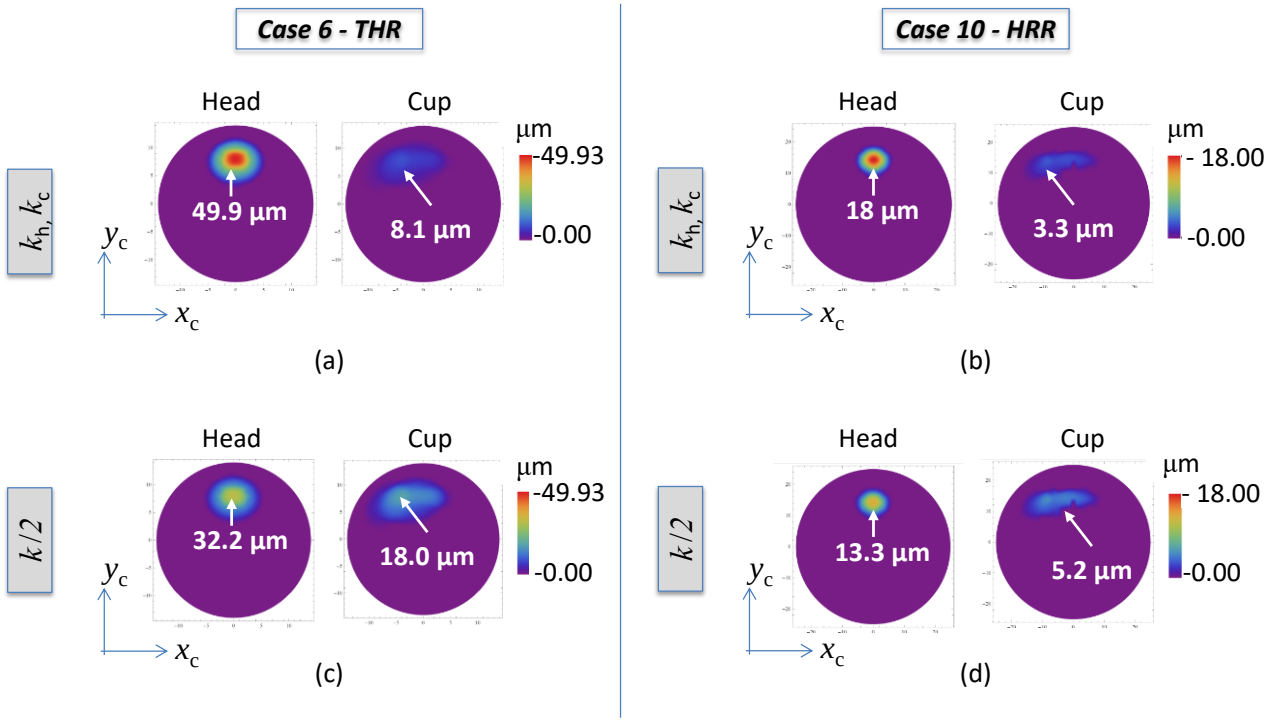

Fig. 5 *Wear maps of cases 6 (a, c) and 10 (b, d) obtained exploiting the distinct wear coefficients for the head and cup (a, b) and the total wear coefficient (c, d). The arrow shows the point where the linear wear depth is at its maximum and reports its value. Note that the wear maps are projected in the plane $x_c y_c$, in the reference configuration.*

5.2. Effect of the implant geometry and the loading conditions on the wear coefficient

As mentioned above, the wear coefficient is a complex parameter that depends on the lubrication regime, and consequently on the implant geometry and materials, the kinematic and loading conditions, and the overall wear process. In this section, the effect of the implant geometry and the loading conditions on the wear coefficient is discussed. To facilitate the discussion, the total wear coefficients of Table 3 are plotted as a function of the head diameter d_h in Fig. 6, which highlights the wide dispersion of k, both for THRs and HRRs, ranging from 0.67 to 9.44 10^{-8} mm^3/(N m) and 2.51 to 7.89 10^{-8} mm^3/(N m), respectively. Such dispersion in the values of k reflects the high sensitivity and hence specificity of the wear coefficient to the test conditions.

First, the effect of the implant geometry (i.e., head diameter d_h and diametrical clearance cl) is discussed. Hip implants with different d_h, but belonging to the same study, were compared; in particular, cases 1-4 [8] and cases 7-8 [16] were examined for THRs and HRRs, respectively. According to the trends depicted in Fig. 6, the larger the head, the lower the wear coefficient. In fact, the comparison between 28 mm vs 36 mm d_h for THRs (case 1 vs. cases 2-4) shows significantly lower k for the larger implant (up to -60%). The same holds for HRRs (case 7 vs. case 8): increasing d_h from 38.5 mm to 54.5 mm determines a 68% reduction of the wear coefficient. This trend can be explained considering the change of the lubrication regime, from the boundary to mixed-full lubrication, for larger implants, also reported in the literature [8]. However, different wear coefficients were calculated for THR and HRR with similar dimensions, as occur for cases 2-4 vs. case 7, most likely due to their different structures and contact mechanics. The effect of the clearance (cl) was also significant. This was clearly revealed by the comparison of cases 2-4, which

involved testing 36 mm implants with clearances in the range of 105 to 143 µm. As depicted in Fig. 6, the decrease of the clearance, which means an increase of contact conformity and hence a better lubrication, caused a decrease of k and h_{max} of approximately 33% and 45%, respectively.

In addition, the effect of the load on the wear coefficient was investigated. In [15], two identical implants were tested under the same kinematics and similar load profiles, only differing for the magnitude of L_{min}, i.e., the swing phase load (100 N for the case 5 vs. 280 N for the case 6). The results show a noteworthy effect of the test load on the wear coefficients: a 3-fold increase of L_{min} causes an almost one order-of-magnitude increase of the wear coefficients and wear depths (red squared marks in Fig. 6).

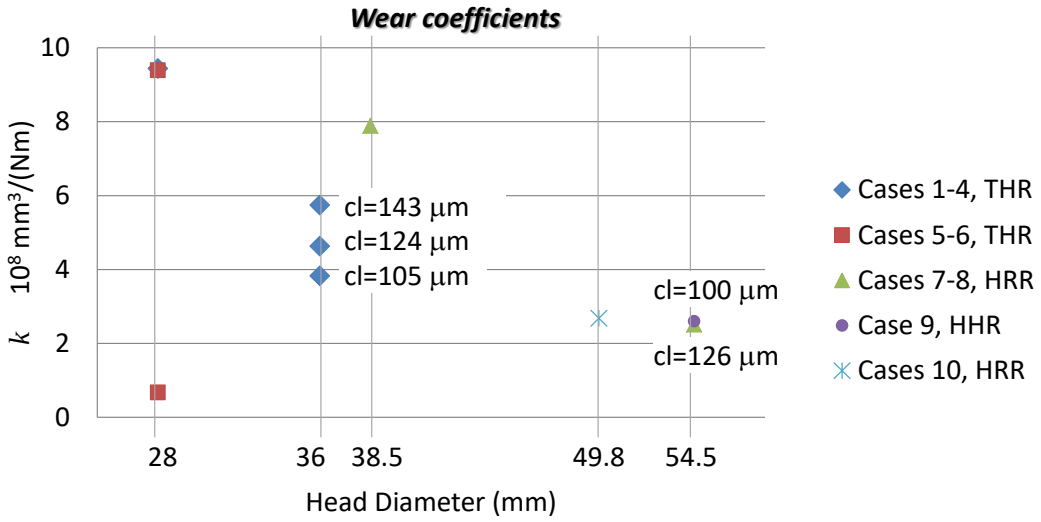

Fig. 6 Plot of the total wear coefficient k as a function of the head diameter, for all simulated cases described in Table 1 (each color refers to a specific study).

5.3. Model limitations

In summary, the wear coefficient is a quantity/function specific of each tribological system and an accurate estimation of k would require both experimental wear data obtained by testing the effective implant conditions, and a numerical model simulating the same test conditions. Consequently, the reliability of the k estimations depends both on experimental data and numerical modeling. In the present study, the former are taken from the literature and thus assumed to be accurate. In contrast, the modeling assumptions of the wear model proposed by the authors are worth discussing. First, neglecting the geometry update can provide good results in the estimation of the volumetric wear and in the shape of the worn regions, but over-estimates the wear depth, as commented in [7,9]. The accuracy of the approximation decreases as wear increases, involving contact pressure redistribution with lower peak values and larger contact area. Second, a frictionless contact was assumed because, according to [7], which simulates the considered Prosim boundary conditions, the presence of friction does not affect significantly the contact pressure and thus the wear volumes that are employed for k estimation. As an example, case 6 was simulated by assuming a coefficient of friction f = 0.2 (Fig. 7). By comparing the frictional and frictionless wear maps (Fig. 7 vs. Fig. 5-a), the former results characterized by wider worn regions and lower wear depths both for the head and cup, up to -40%. Despite the significant differences in the predicted wear depths/maps, almost identical wear coefficients were computed for the two cases, resulting k=9.47 10^{-8} mm^3/(N m), k_c=7.32 mm^3/(N m), and k_h=2.15 mm^3/(N m) for the frictional case (i.e. percentage differences <1.5% compared with the values in Table 2, Case 6 for the frictionless case).

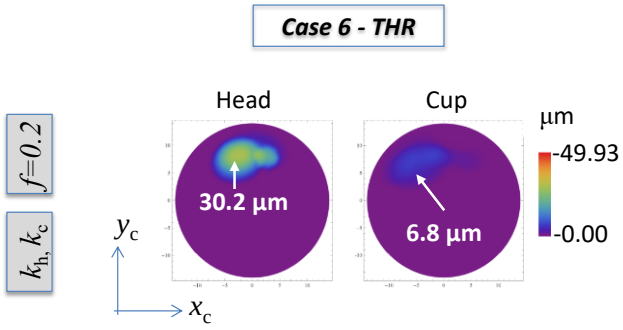

Fig. 7 Wear maps of case 6 obtained exploiting distinct wear coefficients for the head/cup and simulating a frictional contact. The arrow shows the point where the linear wear depth is at its maximum and reports its value. Note that the wear maps are projected in the plane x_cy_c, in the reference configuration.

Regarding the numerical simulations, a key point is the model validation. Frequently, model validation is based on the match between the experimental and the numerical implant total volumetric wear, which, however, is not a real validation if used also for estimating k. To perform such a validation, first, separate wear volumes should be considered for the head and the cup, taking into account the wear redistribution among the two components, as suggested in this study. Second, wear maps should also be taken into account because the same amount of wear volume can be associated to different wear maps. Unfortunately, wear maps are rarely provided in experimental studies performed in hip simulators. The experimental studies mostly report volumetric total wear rates, sometimes combined with optical and scanning electron microscope images of wear defects, surface geometrical features (e.g., roughness) and surface chemical characterization by energy dispersion spectrometry. To the best of our knowledge, only [6] compares numerical wear maps of the cup/head with pictures of the two worn components with the aim of validating the model. However, more quantitative details are necessary to validate the model as well as the assumption of the Archard wear law, which is seldom doubted. Compared to [6], for case 9 in Table 1, our model provided a higher wear coefficient ($1.3\ 10^{-8}$ vs $1.13\ 10^{-8}$ mm^3/(N m)), due to differences in the numerical approaches; in particular in [6] the update of the geometry was implemented. Despite the same volumetric wear and contact pressures in the unworn conditions, different linear wear rates were computed: the values of h_{c/h_max} scaled by k were up to two-fold higher in the present study than in [6]. On the other hand, the predicted wear maps were rather similar in qualitative terms: in both cases the head was affected by a circular worn area located at its pole, while the cup by a stretched damaged region, positioned laterally.

Note that several clinical studies [19,20] provide wear maps of retrieved components, but these cases cannot be simulated with the working conditions being unknown. Consequently, future studies should be addressed to reconstruct implant wear maps also taking advantage of the increasingly widespread use of surface profilometers.

5.4. General remarks on the reliability of the wear coefficients

The set of wear coefficients evaluated in the present work can be used for quick and inexpensive long term wear predictions of implants with characteristics and working conditions identical or similar to those described in Table 1. Indeed, note that a value of k is specific for a given implant working under given conditions. However, this research is not aimed at supplying values of wear coefficients but rather at discussing and suggesting a novel approach to improve both k evaluation and application. Nevertheless, some drawbacks still must be addressed on both the experimental and numerical side. As mentioned above, reliable experimental wear volumes are crucial for accurate k evaluation. A distinct repeatability of the experimental tests is demonstrated by the similar wear coefficients of cases 8 [16] and 9 [6], which reproduced similar test conditions. In contrast, unfortunately, most literature studies reported high variations on V^{exp} measurements of up to 85% [16]. The results also suggest that the wear data from pin-on-disk/plate, often used in the literature, particularly for the metal-on-plastic implants [21,22], can hardly be applied for artificial joint wear assessment. These simplified tests are certainly paramount to investigate particular wear mechanisms, such as the cross-shear of UHMWPE, but they should not be directly applied in the wear modeling of hip implants. Rather, even more realistic conditions should be reproduced in hip wear simulators, going beyond the standard walking cycle, as supported from experimental evidence [23].

Finally, it should be noted that the above discussed wear coefficients, derived from hip simulator tests, should not be applied to simulate *in vivo* conditions; one reason for this is the different fluid lubricating the implant, i.e. human periprosthetic synovial fluid in *in vivo* conditions and diluted bovine serum in hip joint simulators (Table 1). Moreover, the working conditions are much more complex in *vivo* than *in vitro* and can cause wear at the head-neck taper and at the rim of the cup, not considered in the present model.

6. Conclusions

This study investigated the estimation of the wear coefficient of MoM hip replacements from experimental data, and its use in predictive wear models, which can be a powerful tool for HR design and reliability assessment. Indeed, a truthful estimation of k requires itself a validated numerical model and accurate experimental data.

A short background on k estimation is premised, describing the standard procedure applied when only the total wear volume of the implant is available. In this case, a commonly accepted hypothesis in wear modeling of MoM replacements relies on attributing the same wear coefficient to the head and cup. Sometimes, studies in the literature do not clearly specify whether they are using k as the total or the single component wear coefficient, i.e. whether k or $k/2$ value is provided.

To overcome such hypothesis and to generalize the estimation of k for two worn mating surfaces, a novel approach is proposed with its basic analytical formulation, which can be applied to many other tribological system as well. The proposed approach was also implemented in a parametric model developed in Mathematica® by the authors and applied to estimate k from the wear data found in the literature. In seven cases (out of ten examined), such data are limited to a single value of the total wear volume of the head and cup, but in three cases, the separate volumes of the two components are reported. A comparison between the traditional and the novel approach, with single or double k values, respectively, is discussed for the first time in this study. The results indicate that for the simulated conditions, the head wears more than the cup, both in terms of volumetric loss and linear wear depth. On the contrary, the use of a single wear coefficient would have led to the same wear volume for the two elements.

In addition, the influence of the implant geometrical features and the testing conditions on k was investigated. The set of wear coefficients computed for the ten selected cases highlights the high sensitivity of k to the implant

characteristics, i.e., the higher is the head diameter, the lower is the wear coefficient. Similarly, k is strongly affected by the test conditions, as wear is strictly related to the lubrication regime, which in turn depends on the loading and kinematic conditions for a given implant. Therefore, it is not correct to choose k simply on the basis of the material coupling, as the test conditions are important as well. This observation also suggests that wear data from the pin-on-disk/plate is not appropriate for artificial joint wear assessment. Thus, to improve the reliability of the estimation and application of the wear coefficient, it is important to test and simulate the implant in conditions similar to the operating ones. Furthermore, it is suggested that separate wear volumes for the two components should be measured and wear maps should be determined for validating the numerical model.

Ongoing studies aim at improving the numerical model implementing the geometry update due to the wear process. Moreover, the method is going to be applied to MoP implants using the model presented in [14]. Hopefully, with future developments, also some insights of the implant in *vivo* wear will be gained.

References

[1] J. Fisher, Bioengineering reasons for the failure of metal-on-metal hip prostheses: an engineer's perspective, Journal of Bone & Joint Surgery, British Volume, 93-B (2011) 1001-1004.

[2] F. Di Puccio, L. Mattei, Bio-tribology of artificial hip joints, World Journal of Orthopaedics, *In press* (2014) 1-25.

[3] H.S. Gill, G. Grammatopoulos, S. Adshead, E. Tsialogiannis, E. Tsiridis, Molecular and immune toxicity of CoCr nanoparticles in MoM hip arthroplasty, Trends in Molecular Medicine, 18 (2012) 145-155.

[4] L. Mattei, F. Di Puccio, B. Piccigallo, E. Ciulli, Lubrication and wear modelling of artificial hip joints: a review, Tribol Int, 44 (2011) 532–549.

[5] M.N. Harun, F.C. Wang, Z.M. Jin, J. Fisher, Long-term contact-coupled wear prediction for metal-on-metal total hip joint replacement, Proceedings of the Institution of Mechanical Engineers; Part J; Journal of Engineering Tribiology, 223 (2009) 993-1001.

[6] F. Liu, I. Leslie, S. Williams, J. Fisher, Z. Jin, Development of computational wear simulation of metal-on-metal hip resurfacing replacements, J Biomech, 41 (2008) 686-694.

[7] L. Mattei, F. Di Puccio, Wear simulation of metal-on-metal hip replacements with frictional contact, J Tribol, 135 (2013) 1-11.

[8] D. Dowson, C. Hardaker, M. Flett, G.H. Isaac, A hip joint simulator study of the performance of metal-on-metal joints: Part II: Design, J Arthroplasty, 19 (2004) 124-130.

[9] L. Mattei, F. Di Puccio, E. Ciulli, Wear simulation of metal on metal hip replacements: an analytical approach, in: I. C.p.b.P.T. ASME (Ed.) 11th Conference On Engineering Systems Design And Analysis, ESDA 2012, ASME - American Society of Mechanical Engineers, Nantes, France 2012, pp. 555-564.

[10] V. Saikko, O. Calonius, An improved method of computing the wear factor for total hip prostheses involving the variation of relative motion and contact pressure with location on the bearing surface, J Biomech, 36 (2003) 1819-1827.

[11] S. Affatato, M. Spinelli, M. Zavalloni, C. Mazzega-Fabbro, M. Viceconti, Tribology and total hip joint replacement: current concepts in mechanical simulation, Med Eng Phys, 30 (2008) 1305-1317.

[12] J.P. Paul, Forces transmitted by joints in the human body, Proc Inst Mech Eng Part J J Eng Tribol, 181 (1966) 8-15.

[13] F. Liu, J. Fisher, Z. Jin, Effect of motion inputs on the wear prediction of artificial hip joints, Tribol Int, 63 (2013) 105-114.

[14] L. Mattei, F. Di Puccio, E. Ciulli, A comparative study on wear laws for soft-on-hard hip implants using a mathematical wear model, Tribol Int, 63 (2013) 66-77.

[15] S. Williams, D. Jalali-Vahid, C. Brockett, Z. Jin, M.H. Stone, E. Ingham, J. Fisher, Effect of swing phase load on metal-on-metal hip lubrication, friction and wear, J Biomech, 39 (2006) 2274-2281.

[16] I. Leslie, S. Williams, C. Brown, I. Graham, Z.M. Jin, E. Ingham, J. Fisher, Effect of bearing size on the long-term wear, wear debris, and ion levels of large diameter metal-on-metal hip replacements - An in vitro study, Journal of Biomedical Materials Research. Part B, Applied Biomaterials, 87 (Pt B) (2008) 163-172.

[17] C.X. Li, A hip simulator study of metal-on-metal hip joint device using acetabular cups with different fixation surface conditions, Proc Inst Mech Eng H J Eng Med, 225 (2011) 877-887.

[18] D. Dowson, C. Hardaker, M. Flett, G.H. Isaac, A hip joint simulator study of the performance of metal-on-metal joints: Part I: The role of materials, J Arthroplasty, 19 (2004) 118-123.

[19] J.K. Lord, D.J. Langton, A.V.F. Nargol, T.J. Joyce, Volumetric wear assessment of failed metal-on-metal hip resurfacing prostheses, Wear, 272 (2011) 79-87.

[20] W.-C. Witzleb, U. Hanisch, J. Ziegler, K.-P. Guenther, In Vivo Wear Rate of the Birmingham Hip Resurfacing Arthroplasty: A Review of 10 Retrieved Components, J Arthroplasty, 24 (2009) 951-956.

[21] L. Kang, A.L. Galvin, T.D. Brown, J. Fisher, Z.M. Jin, Wear simulation of ultra-high molecular weight polyethylene hip implants by incorporating the effects of cross-shear and contact pressure, Proceedings of the Institution of Mechanical Engineers, Part H (Journal of Engineering in Medicine), 222 (2008) 1049-1064.

[22] L. Kang, A.L. Galvin, J. Fisher, Z. Jin, Enhanced computational prediction of polyethylene wear in hip joints by incorporating cross-shear and contact pressure in additional to load and sliding distance: Effect of head diameter, J Biomech, 42 (2009) 912-918.

[23] M. Hadley, C. Hardaker, S. Williams, Z. Jin, G. Isaac, J. Fisher, Development of a Stop-Dwell-Start (SDS) Protocol for In Vitro Wear Testing of Metal-on-Metal Total Hip Replacements, (2013) 271-291.